General Disclaimer

One or more of the Following Statements may affect this Document

- This document has been reproduced from the best copy furnished by the organizational source. It is being released in the interest of making available as much information as possible.

- This document may contain data, which exceeds the sheet parameters. It was furnished in this condition by the organizational source and is the best copy available.

- This document may contain tone-on-tone or color graphs, charts and/or pictures, which have been reproduced in black and white.

- This document is paginated as submitted by the original source.

- Portions of this document are not fully legible due to the historical nature of some of the material. However, it is the best reproduction available from the original submission.

Produced by the NASA Center for Aerospace Information (CASI)

STATE UNIVERSITY OF NEW YORK

AT STONY BROOK

THERMODYNAMICS AND KINETICS OF REACTIONS

IN PROTECTIVE COATING SYSTEMS

B. Gupta, A. Sarkhel, S. Shankar, L. Seigle

THERMODYNAMICS AND KINETICS OF REACTIONS

IN PROTECTIVE COATING SYSTEMS

B. Gupta, A. Sarkhel, S. Shankar, L. Seigle

Fifth Semiannual Report for the Period

December 1, 1974 to May 31, 1975

TABLE OF CONTENTS

ABSTRACT

Further study of the aluminization of Ni from packs containing various percentages of unalloyed Al confirms that the surface aluminum content of specimens aluminized in such packs tends to decrease with time and consequently a simple parabolic law for the weight-gain vs. time relationship is not obeyed. The diffusivity-composition relationship in NiAl has been re-examined and a new set of curves is presented. A numerical method for the calculation of coating dissolution rates has been developed and applied to NiAl-Ni$_3$Al type of coatings.

I. Introduction

Attention in this project is currently focused on a detailed analysis of the factors influencing the formation and diffusive degradation of aluminide coatings on nickel and cobalt. The kinetics of the pack-aluminization process is under investigation, including a study of diffusivities and layer growth rates of phases in the Ni-Al system. An analysis is being made of coating degradation by coating-substrate interaction, taking into account the complex variation of diffusivites with composition in the Ni-Al system. Progress in the various phases of this project made during the period 12/1/74 - 5/31/75 is given in the following progress report.

II. Boundary Conditions for Diffusion During Pack Aluminizing

Past studies [1] have revealed that the surface compositions of nickel specimens coated in pure Al packs tend to vary with time, thus bringing into question the assumption of time invariant surface composition made in the analysis of the kinetics of pack-aluminization by us as well as Levine and Caves.[2] In order to further investigate this matter, a number of additional experiments were made using AlF_3 activated pure-Al packs with 1 and 4 w/o Al in the packs. The results of these experiments are reported in Tables I C, II C and IV, as well as Figs. 1, 2 and 3.

It will be noted in Figs. 1 and 2 that with 1 w/o Al in the pack the surface composition of specimens aluminized in the AlF_3 activated pack is quite steady at about 44 a/o Al and the w^2 vs. time plot is a fairly straight line through the origin. At 4 w/o Al in the pack the surface composition is high at 1/2 hour but becomes fairly constant between 1 and 20 hours at about 49 a/o Al. The w^2 vs. t plot does not pass through the origin, but shows a rapid weight gain at early times. This type of perturbation is also reflected in the 4 w/o Al, NaF

activated pack (Fig. 2). Therefore, in confirmation of previous observations, it appears that there is an unexpectedly high rate of aluminization in the 4 w/o Al pack at early times, and a simple parabolic relation between weight gain and time is not obeyed.

TABLE I

Weight gain data from pure Al packs at 1093°C, in gms/cm^2

A - Sodium Halide Activators

Time (Hrs.)	1 w/o Al in pack			4 w/o Al in pack		
	NaF	NaCl	NaI	NaF	NaCl	NaI
1	.0054	.0011	.00052	.0086*	.0027	.00107
3	.0071	.0038	.00144	.0268**	.0068	.00335
5	.0080	.0069	---	.0334	.0130	.0049
10	.0114	.0128	.0060	.0425	.0308	.0090
20	.0166	.0181	.0116	.0388	.0389	.0144

B - Ammonium Halide Activators

Time (Hrs.)	1 w/o Al in pack		4 w/o Al in pack	
	NH_4Cl	NH_4I	NH_4Cl	NH_4I
1	.0043	.00016	.00674	.00124
3	.00677	.00027	.00927**	.00333
5	.0076	.00068	.01269	---
10	.0107	---	.01055	.01057

*Coating Time - 1/2 hour
**Coating Time - 2 hours

<center>C - <u>Aluminum Halide Activators</u></center>

Time (Hrs.)	1 w/o Al in pack		4 w/o Al in pack	
	AlF$_3$	AlCl$_3$	AlF$_3$	AlCl$_3$
1	.00465	.0027	.01449	.00881
3	.0068	.00546	.0155	.0090
5	.0086	---	.0152	.0141
10	.0114	.00517	.0196	.0272
20	---	.00815	.02187	.0359

<center>TABLE II</center>

<center>Variation of Surface composition with Time for Pure Al packs at 1093°C (a/o Al)</center>

<center>A - <u>Sodium Halide Activators</u></center>

Time (Hrs.)	1 w/o Al in pack			4 w/o Al in packs			
	NaF	NaCl	NaI	NaF	NaCl	NaI	
1	37.6	49.19	---	53.2*	54.11	47.71[+]	39.3[++]
3	37.0	51.81	---	50.3**	53.02	48.92[+]	33.42[++]
5	37.7	51.48	---	52.0	56.3	48.63	38.42
10	37.4	45.34	42.81	51.0	56.1	47.89	
20	39.5	48.1	43.04	48.8	56.62	47.06	

<center>B - <u>Ammonium Halide Activators</u></center>

Time (Hrs.)	1 w/o Al in pack		4 w/o Al in pack	
	NH$_4$Cl	NH$_4$I	NH$_4$Cl	NH$_4$I
1	49.31	---	53.68	---
3	---	---	52.97**	---
5	50.56	---	52.13	---
10	51.87	---	51.93	45.33[+]
20	---	---	55.63	48.21

*Coating Time - 1/2 hour
**Coating Time - 2 hours

C - Aluminum Halide Activators

Time (Hours)	1 w/o Al		4 w/o Al in pack	
	AlF_3	$AlCl_3$	AlF_3	$AlCl_3$
1	44.11	39.11	48.58	54.00
3	44.47	36.78	49.11	53.89
5	43.77	---	49.67	53.26
10	45.1	38.22	49.38	---
20	---	47.60	49.11	55.32

TABLE III

Weight gain and surface composition data for aluminizing in open and sealed retorts. (4 w/o $AlCl_3$ in open retort and 1 w/o $AlCl_3$ in sealed retort 4 w/o Al at $1093^{O}C$)

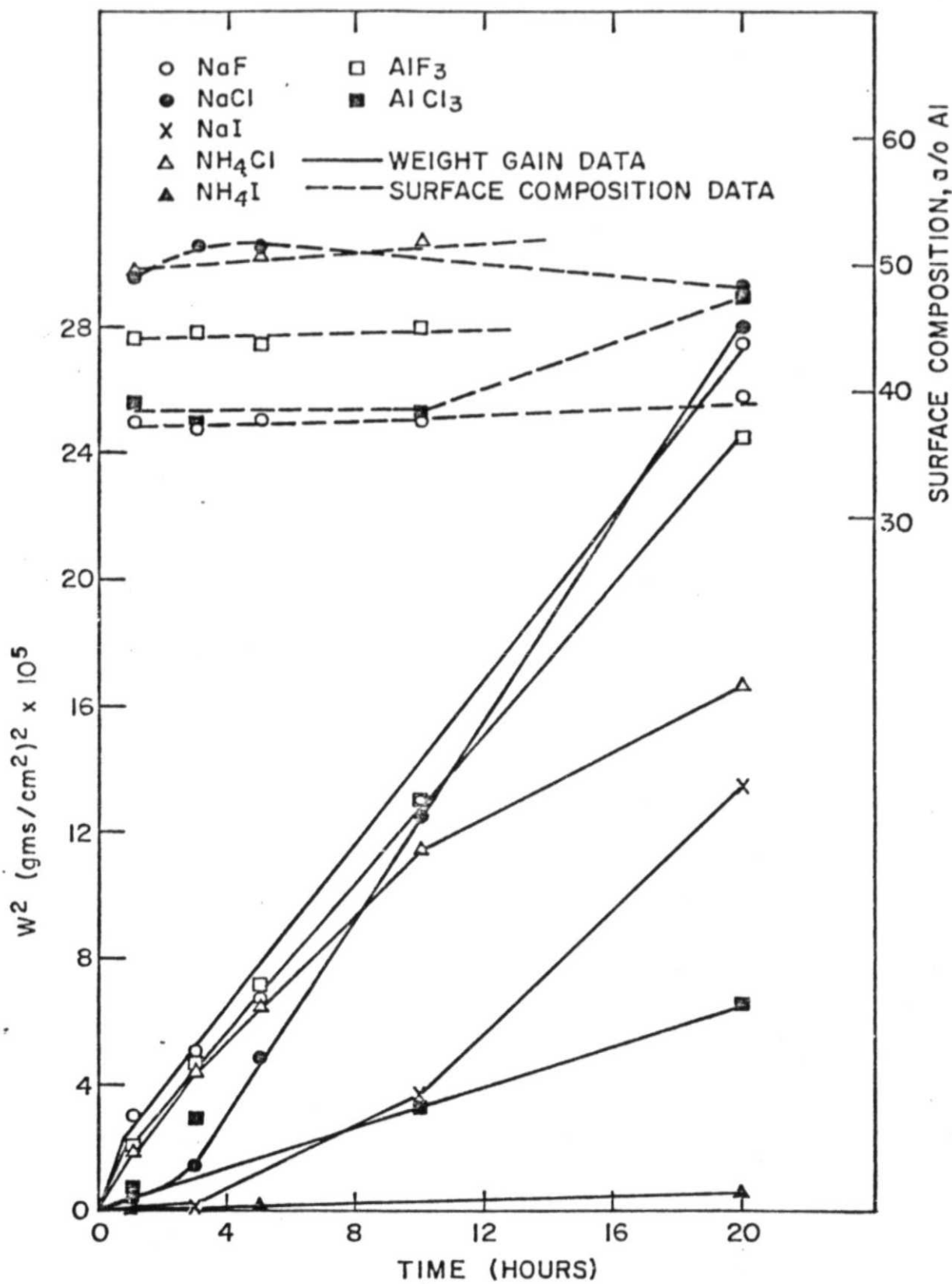| Time (Hours)	Weight Gain, gms/cm^2		Surface Composition, a/oAl	
	Open retort	Sealed retort	Open retort	Sealed retort
1	.0093	.00881	52.96	54.00
3	.0178	.0090	55.3	53.89
5	.0214	.0141	49.45	53.26
10	.0302	.0272	49.41	---
20	.0320	.0359	49.59	55.32

Fig. 1: Surface Composition and Weight Gain Vs. Time in pure Al Packs
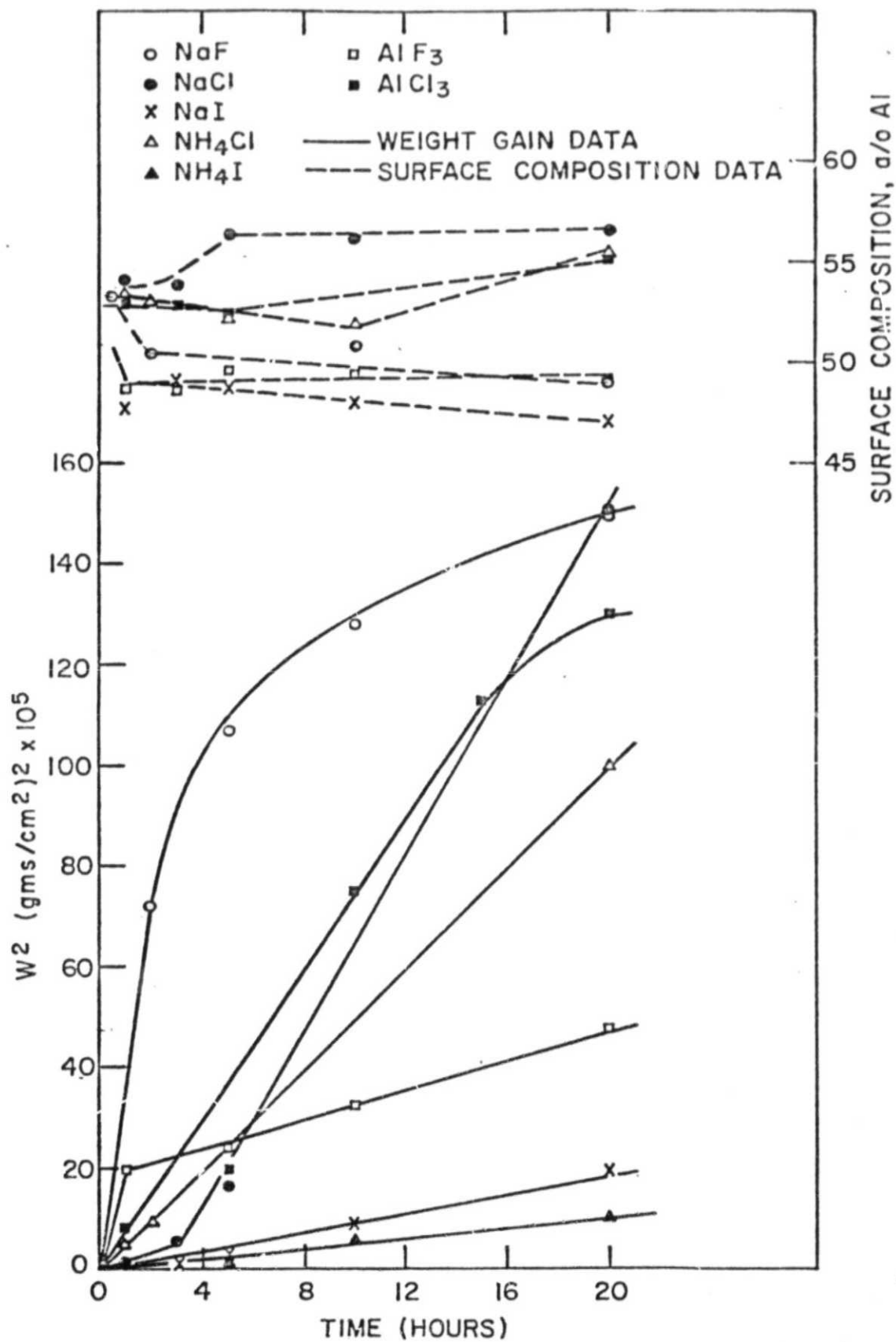(1 w/o Al at 1093°C)

Fig. 2. Surface Composition and Weight Gain Vs. Time in pure Al Packs
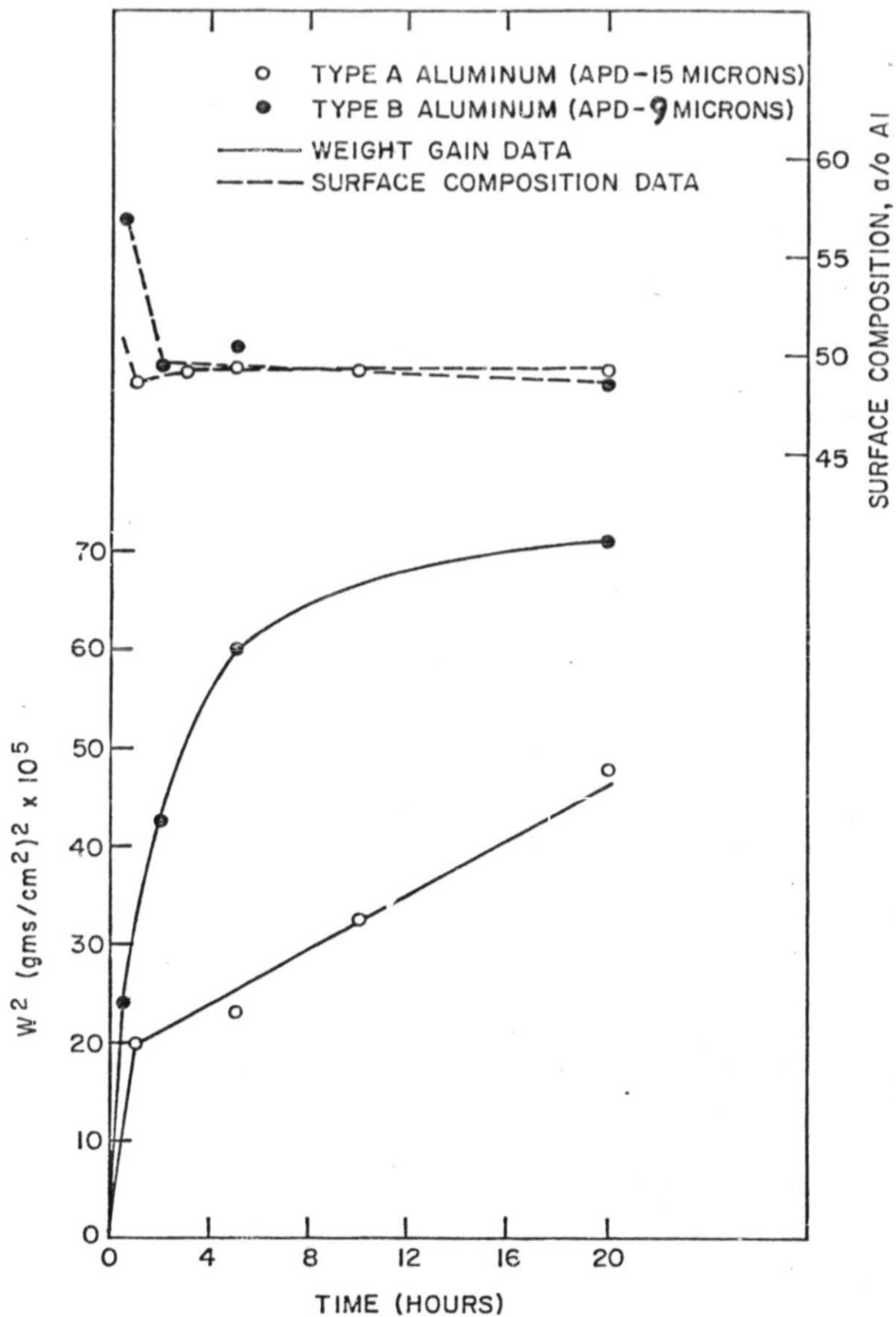(4 w/o Al at 1093°C)

Fig.3: Surface Composition and Weight Gain Vs. Time in pure Al Packs
(4 w/o AlF$_3$, 4 w/o Al at 1093°C)

TABLE IV

Weight gain and surface composition data from AlF_3 activated pure Al packs
(4 w/o AlF_3 at 1093°C)

Time (Hrs.)	Weight gain, gms/cm^2		Surface composition, a/oAl	
	4 w/o Al, Type A	4 w/o Al, Type B	4 w/o Al, Type A	4 w/o Al,Type B
1	.01449	.0157336*	48.58	56.89*
3	.0155	.0205**	49.11	49.3**
5	.0152	.0245	49.67	50.76
10	.0196	---	49.38	---
20	.02187	.0267	49.11	48.61

Type A - Average particle dia. 15 microns

Type B - Average particle dia. 9 microns

*Coating Time - 1/2 hr.

**Coating Time - 2 hr.

The surface composition and w^2 vs. time relationships in 4 w/o Al
packs obtained from this and earlier runs are compared in Fig. 3. It will be
observed that higher surface compositions and weight gains were obtained in
the earlier runs, which used a 9 micron average particle size Al powder, than
in the present runs, which used a 15 micron average particle size Al. In view
of this evidence that Al powder particle size had a strong influence on the
kinetics of the process, a calculation was made of the effect of particle size
on the thermodynamic activity of Al and values of the parabolic rate constant,
Kg, for gaseous transport of Al in the pack, using Levine and Caves formula.
The results show that there is not much change in Kg between 15 and 9 microns,
but a rapid increase in Kg for particle sizes below about 4 microns. These
calculations suggest an explanation of the initially high surface compositions
and rates of weight gain frequently observed in the pure Al packs. That is,
these are due to the presence of a percentage of very fine particles in the

TABLE V

Variation of aluminum activity in pack and aluminum transfer rate
constant with aluminum particle size (4 w/o AlF_3, 4 w/o Al at 1093°C)

| Aluminum Particle size in microns	Aluminum Activity a_{Al}	Aluminum transfer rate constant k_{Al}, $gms^2/cm4.h$	
		For Surface Composition 50 a/o Al	For Surface Composition 55 a/o Al
5	12.2603	22.4600×10^{-3}	22.0740×10^{-3}
1	3.5026	8.7430×10^{-3}	8.5744×10^{-3}
2	1.8716	5.1154×10^{-3}	4.6270×10^{-3}
3	1.2849	3.5370×10^{-3}	3.1390×10^{-3}
10	1.1335	3.0937×10^{-3}	2.8747×10^{-3}
15	1.0870	2.8880×10^{-3}	2.5871×10^{-3}
20	1.0647	2.8212×10^{-3}	2.5233×10^{-3}
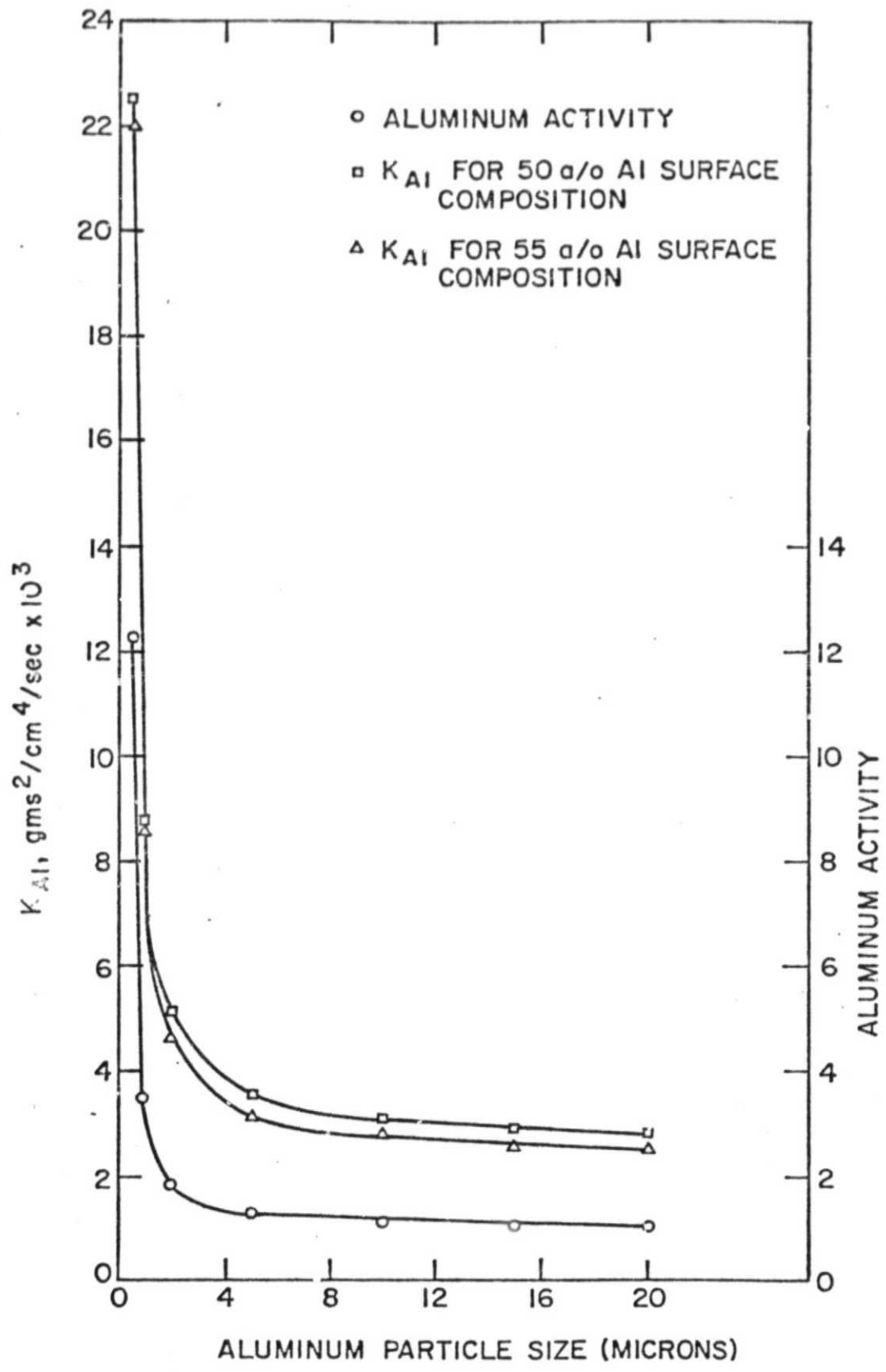
Fig. 4: Variation of Al Activity and Al Transfer Rate Constant with Al Particle Size.

Al powder, which have a high activity. When these particles are used up the Al activity in the pack drops, and also the surface compositions and rates of weight gain. Since the pure Al packs are not pretreated such fine particles could be present initially but disappear quite rapidly as they interact with the activator. If this is true a pretreatment of the Al powder should elininate the fines and experiments with pure Al pretreated packs are being planned.

III. Effect of Activator on Coating Kinetics

Studies of the formation of aluminide coatings on pure Ni using various activators were continued during this report period. Experimental techniques were similar to those used previously in most details. Sealed retorts were used with NH_4Cl, NH_4I, $AlCl_3$ and NH_4I activators, whereas retorts with slide-fitting covers were used with NaCl and NaI as well as AlF_3 and NaF activated packs. The percentages of activator used were the same as those reported in progress report #3 except that 1 w/o $AlCl_3$ was used.

As shown in Tables I and II and Figs. 1 and 2, as observed previously, the sodium and ammonium iodide activators yielded the lowest surface compositions and weight gains (surface compositions for the NH_4I activated packs are not reported due to the poor nature of the surfaces of specimens coated in these packs). However in this series of tests, the chloride activated packs in some instances yielded better results than the fluoride activated packs, in contradiction to past observations. This is particularly evident in the results for the 1 w/o Al packs (Fig. 1) where it will be observed that the highest surface Al content was achieved with the NaCl and NH_4Cl activated packs. According to the weight gain data, NaCl, NaF and AlF_3 performed about alike, with NH_4Cl somewhat less efficient. With the 4 w/o Al packs (Fig. 2) NaCl performed effectively, but the most rapid weight

gains were obtained with NaF as activator. AlF_3 appeared to perform poorly in these tests. It should be noted that NaCl was used in an open rather than sealed retort in these tests.

An important feature of the data is the frequently encountered lack of constancy of surface composition and corresponding departure from linearity of the w^2 vs. time plots. In Fig. 2, particularly, it may be seen that the surface compositions of the fluoride activated packs are high initially but decrease to lower values at later times. Correspondingly, the w^2 vs. t curve possessesa high initial slope, which decreases with time. On the other hand, the NaCl activated pack shows an increase in surface Al content with time, and the slope of the w^2 vs. t plot increases, rather than decreases with time. It is felt that a more direct examination of the processes occurring within the pack is needed in order to explain these results and an effort is being made to examine the pack microscopically after impregnation with a catalytically polymerized epoxy resin. Initial experiments with this technique appear promising.

IV. Correlation of Layer Growth Rates with Diffusivities in the Solid.

A. Variation of Diffusivity with Composition in NiAl.

A few additional runs were made at 1100 and 1150^OC and the entire body of data for the NiAl phase was reanalyzed. According to the recent studies of Taylor and Doyle[3], there can be little doubt that the defect structure of NiAl changes abruptly at almost exactly the stoichiometric composition. The previously reported [1] minima in $\tilde{D}_{NiAl}$ at off-stoichiometric compositions was, therefore, difficult to explain. The composition profiles from which the diffusivity values were calculated show a pronounced inflection in the region of the minima. An example is Fig. 3 of the 2nd Progress Report[4]. Because of the steepness of the slope in this region and difficulty in locating the inflection point exactly, there is some uncertainty in the calculation of D in the vicinity of the inflection. It was decided to recalculate diffusivities assuming that the inflection point was at 50 $^a/_o$ Al and this has led to the more theoretically acceptable $\tilde{D}$ vs. composition curves shown in Fig. 5. The diffusivity values do not differ appreciably in magnitude from those given in Fig. 6 of the last Progress Report, but the shape of the curves around the minima is quite different. Further theoretical analysis of these results is under way.

B. Calculation of Coating Formation and Dissolution Rates.

In our previous progress reports, experimental results and theoretical calculations of growth rates of aluminide layers on nickel substrates were presented. If the composition at the specimen surface remains constant throughout the coating time, the layer thickness of the various aluminide phases can be calculated by solving in a digital computer a system of simultaneous algebraic equations, when the interdiffusion co-efficient is
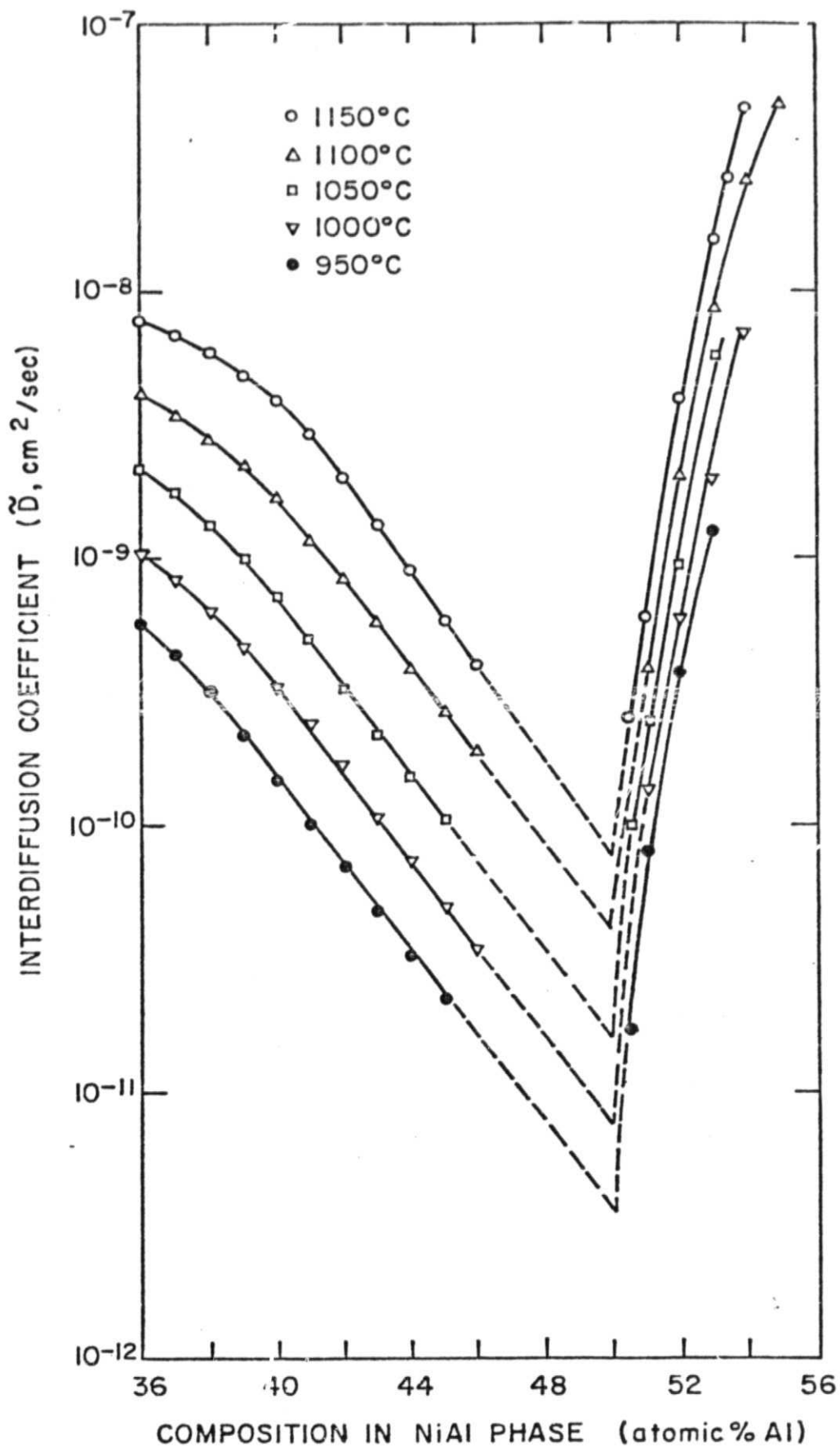
Fig. 5: The variation of $\tilde{D}$ with composition in NiAl

composition-independent [5]. When the interdiffusivities vary with composition, as is the case for NiAl, growth rates can be calculated accurately by numerical methods[6]. These computations have proved valuable in predicting coating thickness and weight-gain as a function of the surface composition of the coating and in comparing the rate of aluminum pick-up by the specimen with the rate of delivery of aluminum by the activated gas-mixture in pack cementation. The latter helps estimate what composition will obtain at the specimen surface, and which phases will form in the coating for different processing conditions. Furthermore, these computations have pointed out that if the nickel substrate contains some alloyed aluminum, as do most nickel-base superalloys aluminide coating formation is somewhat accelerated[1]. It has also been established, by theoretical computation of the growth-rates of NiAl-based coatings, that when the interdiffusion co-efficient in an intermetallic phase is composition-dependent, its over-all growth-rate can be predicted with great accuracy by the use of an integrated-average interdiffusivity, and thus time-consuming numerical solution can be avoided[6]. However, such an approximation fails completely in predicting the composition-profile in that phase, and also causes considerable error in the individual rates of motion of the two interfaces bounding the phase. Consequently, in applications where these are important, numerical solution of the problem, allowing for the composition-dependence of $\tilde{D}$, becomes necessary. A general method of numerical solution, when the interdiffusivity in one or more phases varies with composition, has been developed.

In the light of the above conclusions, a recent publication[7] dealing with formation and dissolution of Ni_2Al_3 coating on pure Ni can be critically examined. In this study, nickel specimens were coated at $870^{\circ}C$, $900^{\circ}C$ and

$1000^{\circ}C$ for various lengths of time in NH_4Cl - activated packs containing 15 w/o pure Al. The coating consisted predominantly of Ni_2Al_3 on the surface, with a thin layer of NiAl beneath it. Theoretical calculation of the coating growth-rate using the interdiffusion co-efficients of Ni_2Al_3, NiAl, Ni_3Al and the Ni(Al) solid solution available in the literature, did not correspond with the experimental results. The authors pointed out that the values of the interdiffusion co-efficients derived from the literature are questionable. $\tilde{D}_{NiAl}$ was available in the temperature range of interest (870-$1000^{\circ}C$), but they are inaccurate because Al-excess NiAl resembles Ni_2Al_3 in appearance, and thus had led to improper identification, and consequent errors in diffusion studies. For the Ni_2Al_3 (γ) phase, the interdiffusion coefficients were obtained by extrapolating values determined at $600^{\circ}C$, and, as a result, could have had imposed low temperature effects e.g. grain-boundary diffusion. Therefore, the authors determined effective $\tilde{D}$ for Ni_2Al_3 and NiAl by fitting the experimental layer-growth data to model calculations. The effective values of $\tilde{D}_{NiAl}$ thus obtained (denoted D_R here) correspond well with our integrated composition-average interdiffusivity ($\bar{D}$) for NiAl ($D_R = 3.1 \times 10^{-9}$, $\bar{D} \simeq 3 \times 10^{-9}$ cm^2/sec at $1000^{\circ}C$; $D_R = 6.3 \times 10^{-10}$ cm^2sec at $930^{\circ}C$, $\bar{D} \simeq 6 \times 10^{-10}$ cm^2/sec at $950^{\circ}C$). They also obtained $D_{Ni_2Al_3}$ by this regression analysis. These values were a factor of 2 to 3 smaller than those obtained by the entrapolation of the data in Ref. 8. It should be considered that the authors made an important assumption for these calculations, namely that the surface composition of the $Ni_2Al_3(\gamma)$ coating corresponds with the maximum solubility of Al in γ, and also that this composition was time-invariant. Constancy of surface composition appears to have obtained, after a short incubation period, because the growth of the Ni_2Al_3 was found to be parabolic at all coating temperatures. However, the assumption

that the surface composition corresponded with the high Al limit of γ at any temperature has not been experimentally verified. In our coating experiments, it has been shown that the surface composition depends on the nature of the pack as well as on temperature. The single-phase γ-field is only about 3-4 a/o Al wide in temperature range of interest. If the actual surface composition of the Ni_2Al_3 phase were up to 2 a/o Al less than what has been assumed in the study reported in Ref. 7, the inter-diffusion coefficients deduced would be higher by nearly a factor of 2 than the reported values, and will move closer to the data of Ref. 8. Since the coating formed at these low temperatures was predominantly Ni_2Al_3, the effect of such an error on $\bar{D}_{NiAl}$ will be small, and we believe that the effective $\bar{D}_{NiAl}$ derived from the layer growth data is accurate.

The second part of the study was concerned with the homogenization and eventual dissolution of the $Ni_2Al_3(\gamma)$ phase, and consequent growth of the underlying NiAl(δ) Phase, when the specimens are removed from the pack environment and annealed at high temperature (Step 2). Homogenization experiments were carried out also at $870^\circ C$, $930^\circ C$, $1000^\circ C$. Finite difference numerical solution of the system of partial differential equations subject to the boundary conditions appropriate to the process was carried out to simulate the phase-boundary movement during this step. $\bar{D}_{Ni_2Al_3}$ and $\bar{D}_{NiAl}$ required for the theoretical simulation were those determined from the layer growth data in the former step. The growth of the δ-layer predicted by the numerical solution agreed closely with the experimental results (See Fig. 7 in Ref. 7). It was also found that certain analytic approximations could predict the δ-growth rate very accurately. The basic premise of these approximations is the same that we advanced in Progress Report #1 (pp. 32-38)[5] regarding the behavior of NiAl-Ni_3Al coatings when put into service. The surface layer of the coating--the Ni_2Al_3 phase in Ref. 7--homogenizes rapidly, if its

diffusivity is high and its composition range, $(c_s - c_1)$ small. The time of homogenization (t_h) of the γ-layer, of initial thickness X_γ^0 can be estimated by dividing the excess aluminum content, approximately $\frac{1}{2}(c_s - c_1)X\gamma^0$, by the average flux $\frac{1}{2}\tilde{D}\gamma(c_s - c_1/X\gamma^0$ through the $\gamma\delta$ interface, assuming that during this period, the thickness of γ does not change significantly:

$$t_h \simeq X_\gamma^{0^2}/\tilde{D}\gamma$$

The numerical results were similar--

$$t_h \simeq 1.15\ X_\gamma^{0^2}/\tilde{D}\gamma \ \text{at} \ 870^\circ C$$

$$t_h \simeq 0.95\ X_\gamma^{0^2}/\tilde{D}\gamma \ \text{at} \ 930^\circ C$$

$$t_h \simeq 0.55\ X_\gamma^{0^2}/\tilde{D}\gamma \ \text{at} \ 1000^\circ C$$

The numerical solution indicated that once the concentration-gradient in the Ni_2Al_3 (γ) layer is homogenized, subsequent growth of the NiAl (δ) layer is parabolic, as expected. Therefore, the numerical scheme can be terminated after homogenization and the rate constants for the movement of the $\gamma\delta$ and $\delta\varepsilon$ interfaces can be calculated analytically, as in the case of coating formation. Even though the interdiffusion coefficient in the δ-phase is known to be composition-dependent, Hickl and Heckel's results show that the use of an average interdiffusivity predicts the overall growth-rate of δ accurately. However, as we have mentioned previously, there may be errors in the individual rates of the movement of the $\delta\varepsilon$ and $\gamma\varepsilon$ interfaces. The movement of the $\delta\varepsilon$ interface determines the dissolution kinetics of the Ni_2Al_3 (γ) layer. The authors have not given their computational results for γ-phase dissolution.

One of the mechanisms of degradation of protective coatings during service at high temperature is interdiffusion of the coating with the substrate material. The theoretical prediction of coating dissolution rates, taking into account the initial concentration-profile inherited

from the coating process as well as the variation of D with composition in the phases constituting the coating, is a problem of general importance in this area. A method of calculation will be briefly described, and some results presented for NiAl(δ)-Ni$_3$Al(ϵ) type of coatings on pure nickel substrate. It is assumed that this type of coating was formed under the condition of constant surface composition (c_s). The surface composition and the length of time of pack cementation at a particular temperature determine the thicknesses of the NiAl and Ni$_3$Al layers and the concentration-profile across the diffusion-zone that exists in the coating. These parameters are calculated by our growth rate scheme[6], and used as initial conditions (t=o, see Fig. 6a) for the next step, namely, the homogenization and dissolution of the NiAl layer, and growth of Ni$_3$Al, by interdiffusion, as the coated component is put into service. In this idealized model of coating degradation by interdiffusion, loss of aluminum by evaporation and oxidation is not considered. Therefore, the important boundary condition for this step is that the coating surface is stationary and the flux of Al (or, Ni) out of the surface in zero. The other boundary condition of maintenance of equilibrium compositions at the interfaces is the same as in coating formation. Distance is measured from the stationary coating surface, and compositions are expressed in atomic fraction aluminum.

The change in composition at any point is expressed as a total differential:

$$dc = \left(\frac{\delta c}{\delta x}\right)dx + \left(\frac{\delta c}{\delta t}\right)dt$$

i.e.
$$\frac{dc}{dt} = \left(\frac{\delta c}{\delta x}\right)\frac{dx}{dt} + \left(\frac{\delta c}{\delta t}\right) = \left(\frac{\delta c}{\delta x}\right)\frac{dx}{dt} + \frac{\delta}{\delta x}\left(D\frac{\delta c}{\delta x}\right)$$

The last term in the equation above comes from the diffusion equation or Fick's Second Law. Such an equation holds for each of the δ, ε and ζ phases. The last term can be simplified depending on whether D = D(c), as in NiAl, or whether D $\neq$ D(c) as in Ni_3Al and Ni(Al):-

$$\frac{dc}{dt} = (\frac{\delta c}{\delta x}) \cdot \frac{dx}{dt} + D \frac{\delta^2 c}{\delta x^2} + \frac{\delta D}{\delta c}(\frac{\delta c^2}{\delta x}) \qquad \text{for NiAl} \quad \ldots(1)$$

$$\frac{dc}{dt} = (\frac{\delta c}{\delta x}) \frac{dx}{dt} + D \frac{\delta^2 c}{\delta x^2} \quad \text{for } Ni_3Al \text{ and Ni(Al)} \quad \ldots(2)$$

The numerical solution is carried out by a procedure similar to that used by Hickl and Heckel[7]. Each phase is divided into a fixed number of equidistant nodes, the distance between any two nodes in a phase being equal to a certain fraction (0.1) of the instantaneous phase thickness. Since the solid solution Ni(Al) phase is infinitely extended, a boundary is imagined at a low enough composition (1 a/o Al), and assumed to move parabolically during homogenization of the surface layer, δ, at a rate which is the average between its rates of movement during coating forma-tion and after NiAl - homogenization (Fig. 6b). The above equations can be written in finite differences and solved to obtain the concentration-profile in the coating at the beginning of any time-step. Thus, for a node n in the NiAl(δ) phase at the time-step (j+1):-

$$(c_{n,\,j+1} - c_{n,j})/\Delta t = \frac{(c_{n+1,j} - c_{n-1,j})}{2\Delta x_1} \cdot \frac{n-2}{p-2} \cdot \frac{(l_{1,j+1} - l_{1,j})}{\Delta t}$$

$$+ D_\delta(c_{n,j}) \cdot \frac{(c_{n+1,j} - 2c_{n,j} + c_{n-1,j})}{\Delta x_1^2} + \frac{D_\delta(c_{n+1,j}) - D_\delta(c_{n-1,j})}{(c_{n+1,j} - c_{n-1,j})} \cdot$$
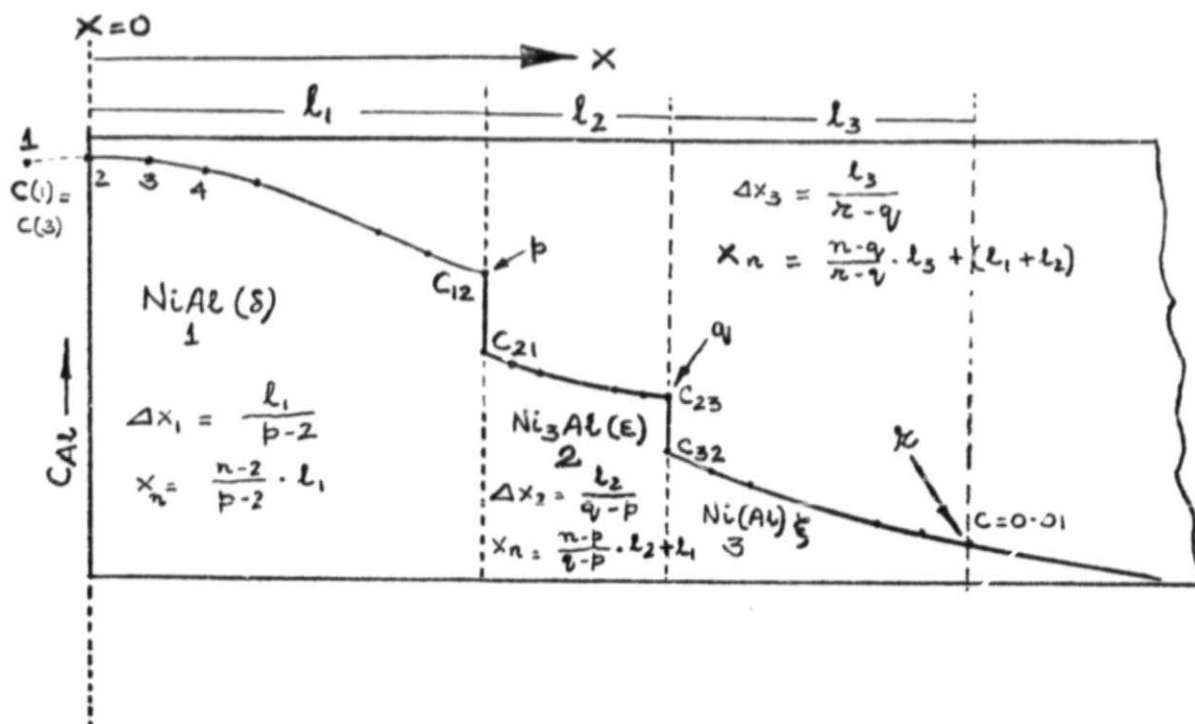
$$\{\frac{c_{n+1,j} - c_{n-1,j}}{2\Delta x_1}\}^2$$

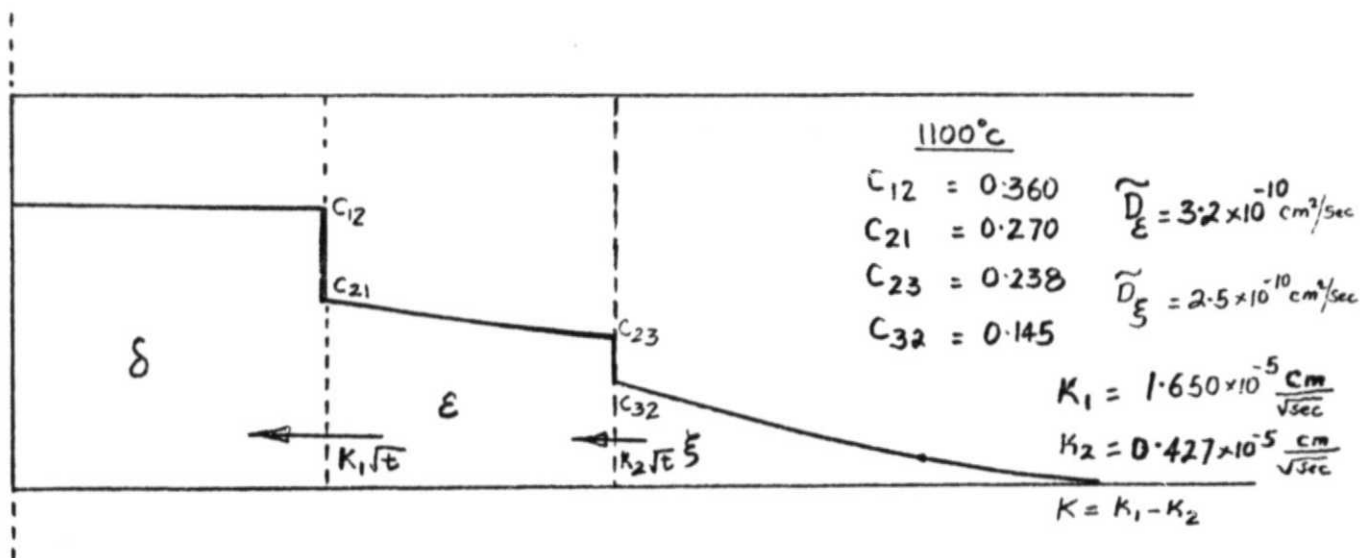Fig. 6(a): The structure of NiAl - Ni₃Al coating (schematic) at t=o and the terminology for numerical solution.

Fig. 6(b): The structure of the coating after homogenization of the NiAl layer $(t=t_h)$.

Two such equations also hold for the ε and ζ phases, the only difference being that for the latter phases, the last term in the above equation drops out and $\tilde{D}$ in the second term is composition-independent. It is to be noted that in order to solve eq. (3), the layer thickness, $l_{1,j+1}$ at the time-step $(_{j+1})$ has to be known. This is obtained by a mass balance at the interface, e.g. for the $\delta\varepsilon$ interface:

$$l_{1,j+1} - l_{1,j} = \frac{\Delta t}{c_{12} - c_{21}} \{ D_\delta(c_{12}) \cdot \frac{c_{12} - c_{p-1,j}}{\Delta x_1} + D_\varepsilon \cdot \frac{c_{p+1,j} - c_{21}}{\Delta x_2} \}$$

Note that both Δx and Δt are variable:

$$\Delta x_{1,j} = 0.1(l_{1,j}) \; ; \; \Delta x_{2,j} = 0.1(l_{2,j}) \; ; \; \Delta x_{3,j} = 0.1(l_{3,j})$$

and $\Delta t(j,j+1) = \min (\Delta x_1^2/4D_\delta(c_{12}) , \Delta x_2^2/4D\varepsilon , \Delta x_3^2/4D_\zeta)_j$

The layer thicknesses and the concentration-profile can be calculated at intervals of time as the δ-phase progressively homogenizes. Denote the time of homogenization by t_h, and the NiAl and Ni_3Al thicknesses at this time by l_{1h} and l_{2h} respectively (see Fig. 6b). Further movement of the $\delta\varepsilon$ and $\varepsilon\zeta$ interfaces will be parabolic, and it can be shown that for $t > t_h$:

$$l_1 = l_{1h} + (\frac{k_1}{k}) l_{2h} - k_1 \{ t - t_h + (l_{2h}/k)^2 \}^{\frac{1}{2}} \quad \cdots\cdots(3)$$

$$l_2 = k \{ t - t_h + (l_{2h}/k)^2 \}^{\frac{1}{2}} \quad \cdots\cdots(4)$$

k_1, k_2 and k are calculated by the coating growth-rate model [6]. The layer thicknesses of NiAl and Ni_3Al in the coating as a function of time during service at $1100^\circ C$ were calculated, employing the numerical
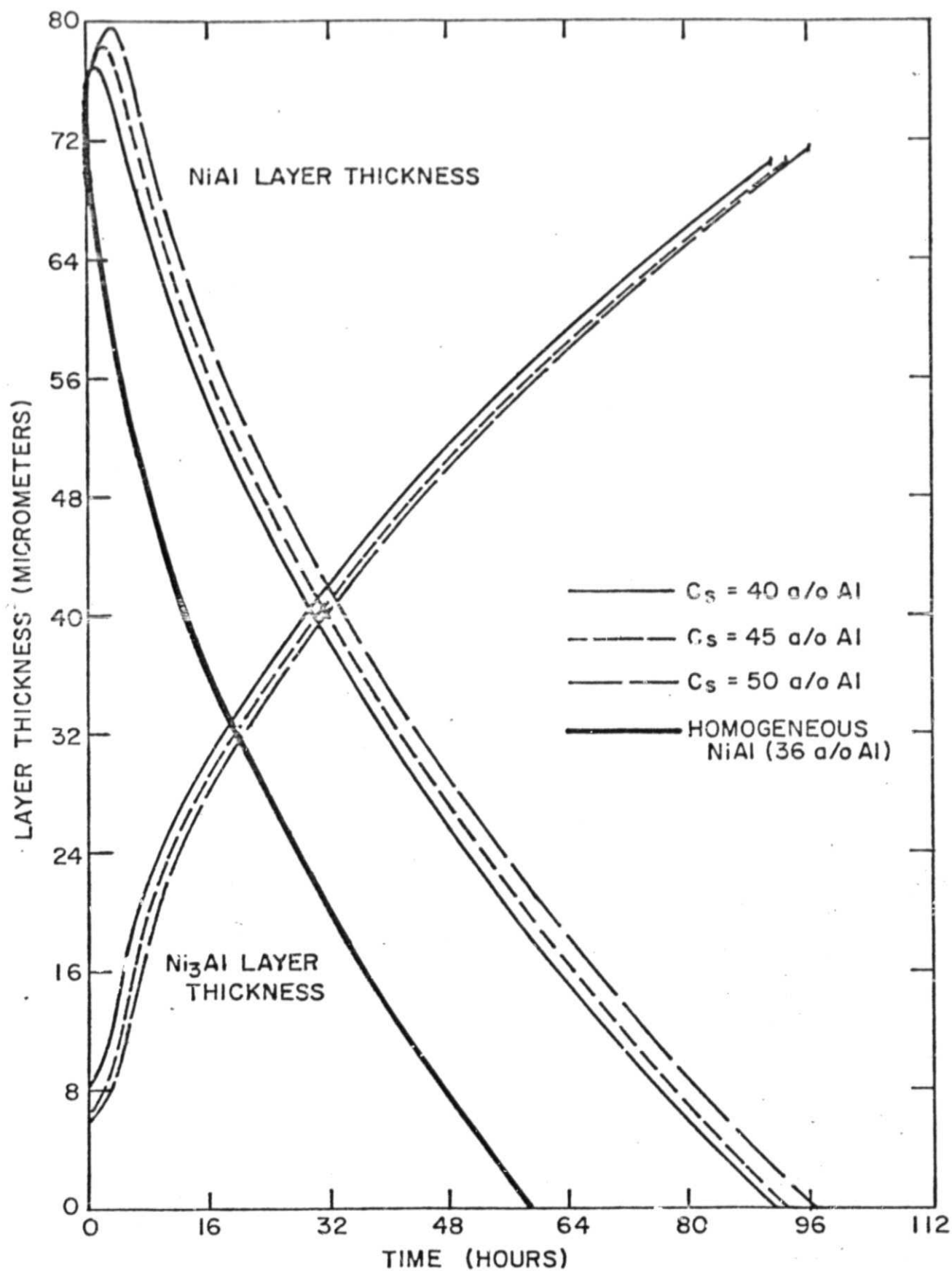
Fig. 7: The variation of NiAl and Ni₃Al thicknesses as a function of exposure time at 1100°C (calculated, initial NiAl thickness 3 mils)
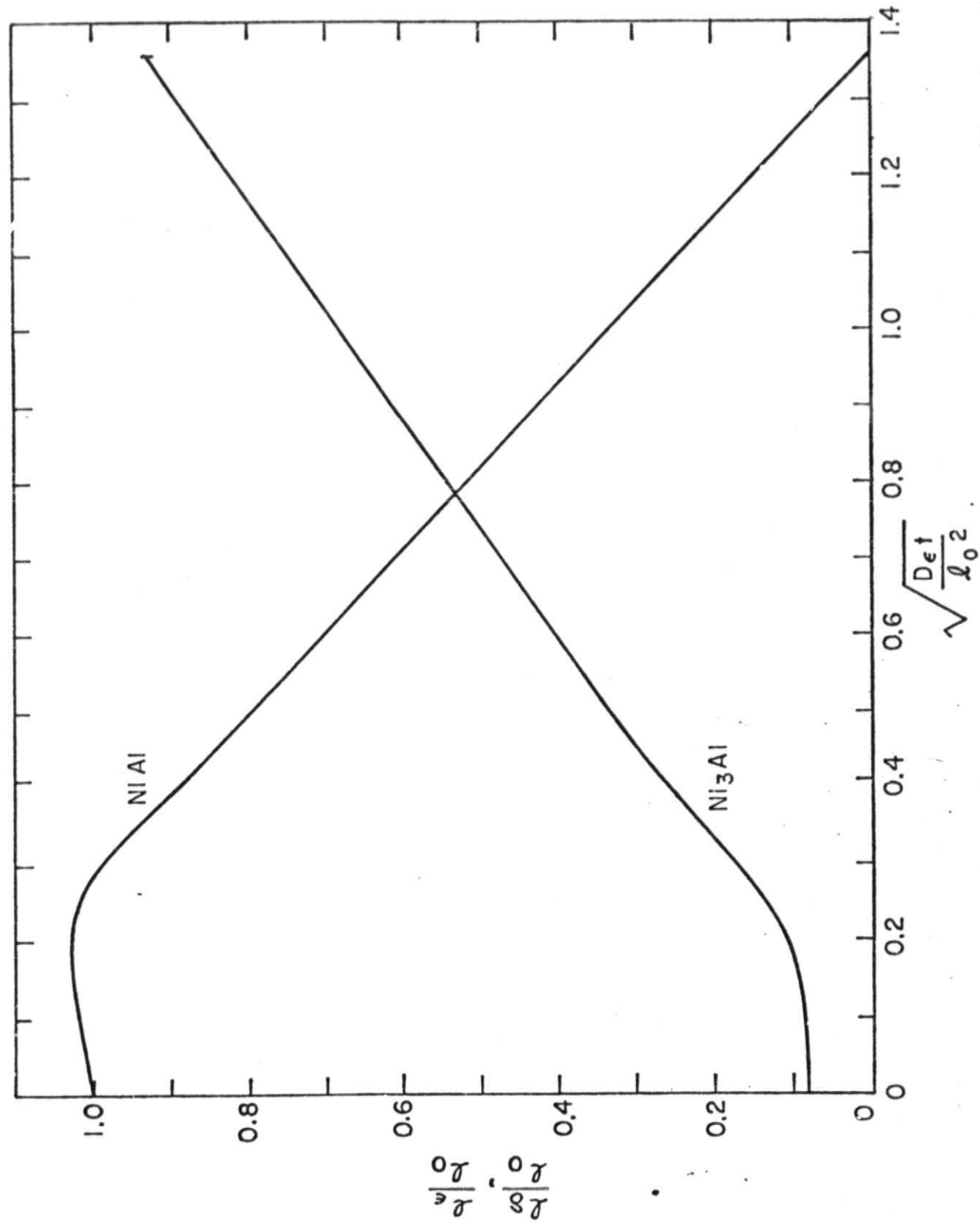
Fig. 8: The variation of instantaneous NiAl (l_ϵ) and Ni$_3$Al (l_s) thicknesses as a function of dimensionless time at 1100°C (calculated for C_s = 45 a/o Al, $\tilde{D}_\epsilon$ (1100°C) = 3.2 x 10^{-10} cm^2/sec; lo = initial NiAl thickness)

scheme during homogenization of δ, and by eq. (3) and (4) after homogenization. The results are given in Fig. 7 and 8. Initial surface compositions investigated were 40, 45, 50 and 36 a/o Al -- the last corresponding to an initially homogeneous (and therefore the least protective) NiAl for which the numerical solution was not necessary. The results given in Fig. 7 correspond to a starting NiAl thickness of 76.2 µm or 3 mils in all cases. The Ni_3Al thickness that is associated with a 3 mil NiAl layer depends on the surface composition of the coating. It is observed that the initial concentration-gradient in the coating leads to a transient non-parabolic kinetics during homogenization of the NiAl layer, following which the dissolution of the NiAl and growth of the Ni_3Al layers are parabolic. This adds to the life of the protective NiAl layer -- increasing it from about 60 hr. for the homogenous NiAl to about 100 hr. for the NiAl layer with a surface composition of 50 a/o Al. It is interesting that for a given initial surface composition, the dissolution kinetics can be expressed in terms of dimensionless parameters only, as in Fig. 8. This obviates the necessity of a new set of computations for a different starting NiAl thickness. As an example, if the NiAl layer with an initial surface composition of 50 a/o Al were 5 mils thick, it would dissolve by interdiffusion completely in $100.(5/3)^2 = 278$ hr.

The accuracy and convergence of the numerical method will be investigated by varying the node spacing and time step-size, and an attempt will be made to develop suitable approximations for the homogenization step. This scheme will be applied to coatings which are formed on nickel substrates containing aluminum in solid solution, for which case, our preliminary calculations have indicated (Ref. 5, pp. 32-38) that coating life is substantially increased.

V. Future Work

A. Kinetics of Pack Aluminization

Results obtained with the pure Al packs indicate that there are complexities in the aluminization process not yet well understood. In order to improve our picture of behavior in the pack it appears that it will be necessary to study the pack more directly, and this is a principal objective of the next phase of our work. A possible technique is impregnation of the pack with a self-hardening resin and microscopic examination. This would enable a determination of the exact type and distribution of pack constituents at various phases of the coating process and thus permit a check of the assumptions of the Levine and Caves model. Preliminary results with this technique appear promising and it will be pursued in detail in the coming months.

B. Correlation of Rates of Coating Formation with Diffusional Properties of the Solid.

Experimental work will continue on a study of the diffusional parameters of phases in the Ni-Al system. The next objective is to determine the ratio of intrinsic diffusivities D_{Ni}/D_{Al} as a function of composition. Initial investigations indicate that this can best be accomplished by a study of the motion of fiduciary markers in pack-aluminized specimens and this technique will be studied in detail during the next period. In addition, with aid of the recently determined interdiffusion coefficients a fairly complete theoretical description of coating formation rates will be mapped out as an aid to workers in the field.

C. Coating - Substrate Interaction

The theoretical calculation of coating dissolution rates will be continued, applying the numerical method outlined here to various types of coatings in the Ni-Al System in the temperature range 800 - 1200°C. An experimental study will be made of actual diffusive degradation rates, and the effects of non-ideal conditions such as grain-boundary diffusion will be ascertained.

REFERENCES

1) Fourth Semiannual Report for the period 6/1/74 - 11/30/74, NASA Research Grant NGR-33-015-160

2) S.R. Levine and R.M. Caves: J. Electrochem. Soc., Vol. 121, 1974, P.1051

3) A. Taylor, N.J. Doyle: J. Appl. Crystallography, Vol 5, 1972, p.201.

4) Second Semiannual Report for the period 6/1/73 - 11/30/73, NASA Research Grant NGR-33-015-160

5) First Annual Report for the period 6/1/72 - 5/31/73, NASA Research Grant NGR-33-015-160

6) Third Semiannual Report for the period 12/1/73 - 5/31/74, NASA Research Grant NGR-33-015-160

7) A.J. Hickl and R.W. Heckel: Met. Trans., Vol. 6A, 1975, p.431

8) L.S. Castleman and L.L. Seigle: Trans. TMS-AIME, Vol. 212, 1958, p.589